Hydropower reservoir management using multi-factor price model and correlation between price and local inflow

Joakim Dimoski[a], Sveinung Nersten[a,*], Stein-Erik Fleten[a], Nils Löhndorf[b]

[a]*Norwegian University of Science and Technology, Norway* , [b]*Vienna University of Economics and Business, Austria*

Abstract

Hydropower producers with reservoir capacity have a special challenge when it comes to weighing the short-term profit from selling power in the day-ahead spot market against waiting for better electricity prices. In this paper, we propose a medium-term scheduling model for a price-taking hydropower producer, using a horizon of two years. We use the price of forward contracts to forecast future spot prices, and use multiple factors to describe movements in price. Further, we include a short-term correlation between movements in electricity price and local inflow. Our main contribution is a comparison of the performance of our scheduling model to a model in which price and local inflow are assumed to be independent and a model in which price movements are described using only one factor. We quantify the loss in expected revenues of using the latter two models compared to ours when price movements are in fact driven by multiple factors and correlated with local inflow. In both cases, we find the loss to be approximately 2-3 %. We have based our study on a Norwegian hydropower plant.

Keywords: Hydropower reservoir management, Markov decision process, multi-factor price process, price and local inflow correlation, stochastic dynamic programming

1 Introduction

The decision problem of hydropower producers, which seek to dispatch the water in their reservoir optimally, has existed for many years, and multiple approaches for formulating and modelling such problems have been proposed. Massé (1946) argues that deterministic models are not good enough, as they do not incorporate the flexibility a production planner has when it comes to the timing of production. Instead, one should use a flexible approach which can provide the hydropower producer with optimal decision policies for both the current and future states of the world, incorporating the uncertainty in future states. The flexible approach proposed by Massé (1946) is still relevant for how reservoir management is performed today.

Inspired by Massé (1946) and multiple papers of more recent date, we aim to create a dynamic scheduling model for a price-taking hydropower production planner that participates in a deregulated power market. The planner operates a plant that is assumed to be sufficiently small so that the decisions of the production planner do not affect the market as a whole. We also assume that the production planner only participates in the spot market. Further, we consider two stochastic variables (spot price and inflow) and we use a time horizon of two years and weekly granularity which is suitable for medium-term planning. This is in compliance with multiple current models for medium-term reservoir management, as described in Iladis et al. (2008), Wolfgang et al. (2009) and Abgottspon and Andersson (2014).

Our contributions in this work include the use of a multi-factor price process, as opposed to existing models for reservoir management which often use single-factor processes to describe movements in price. We include a correlation coefficient between changes in price and local inflow, thereby treating them as dependent variables. Further, we quantify the loss in expected revenues if they assume price and local inflow to be independent when they are in fact correlated, and equivalently, the losses that occur if they use a single factor price process when price movements are in fact described by multiple factors.

To obtain optimal decision policies in each discrete state for the production planner, one can use stochastic dynamic programming as introduced by Bellman (1957). An issue with dynamic programming is the so-called curse of dimensionality, that is, the problem might become too difficult to solve when the state space and number of decision variables become too large. In order to avoid this, Pereira and Pinto (1991) introduce an algorithm for stochastic dynamic programming, a solution approach known as stochastic dual dynamic programming (SDDP). SDDP and similar approaches are widely used in existing literature on hydropower production scheduling, e.g. in Mo et al. (2001) and Rebennack (2015). Löhndorf et al. (2013) introduce a framework that integrates SDDP with Markov processes, referred to as approximate dual dynamic programming (ADDP). Given a current state of the world, the next state value of a variable following a Markov process is only dependent on its current state value, and not its entire history. Similarly, in a Markov Decision Process (MDP), all

*Lead author. Kolbjørn Hejes vei 1E, 7034 Trondheim, Norway. +47 458 23 304. sveinung.nersten@gmail.com

decisions are made based on the current state of the world and its future expected states, irrelevant of all past states.

Multiple authors, e.g., Lamond and Boukhtouta (1996), show that it is reasonable to treat hydropower reservoir management problems as MDPs, an approach we adopt in this paper. We therefore treat inflows and price movements as Markov processes, and use a scenario lattice to discretize all future states and transition probabilities. To construct the lattice, we use the method proposed by Löhndorf and Wozabal (2017). We also use their method for solving stochastic dynamic programs, ADDP, to obtain all optimal decision policies.

We incorporate two stochastic state variables; spot price and inflow. EOPS (SINTEF, 2017b), which is one of the most common commercial programs for medium-term reservoir management for smaller systems in the Nordic countries, uses spot price scenarios generated using EMPS (SINTEF, 2017a). EMPS is a fundamental model which, among others, can forecast spot prices in larger power systems by using historical scenarios of stochastic variables like area inflow and demand (Wolfgang et al., 2009). Mo et al. (2001) show that there is a high correlation between the prices of successive weeks simulated using EMPS. Therefore, until 2000, EOPS used an AR(1) process (a single-factor model) to describe the price movements found by EMPS, illustrated in Flatabø et al. (1998). As shown in Mo et al. (2000), price scenarios in EOPS are still generated using EMPS, but the prices are now organized in a lattice using the scenarios directly instead of expressing them with an autoregressive process.

In contrast to how spot price scenarios are generated in EOPS, we generate them using movements in the price of forward contracts traded in the market. These movements are modelled using a multi-factor model, commonly referred to as an HJM model (Heath et al., 1992). Clewlow and Strickland (2000), Koekebakker and Ollmar (2005) and Bjerksund et al. (2008) argue that one-factor models such as AR(1) are unrealistic for accurately representing forward and spot price movements. Instead, they propose using multi-factor models, which according to them give a much more realistic representation of the dynamics behind price movements. Like Koekebakker and Ollmar (2005), we find the coefficients of the price process empirically by first constructing forward curves for many consecutive trading days, and then calculate daily deviations between the curves and use PCA to obtain multiple factors.

The other stochastic variable we consider is inflow. When determining the characteristics of the inflow, there are several questions that must be answered - whether the system is a local or a regional system consisting of a number of power plants, if there is a seasonal pattern to the inflow, if there are rain periods or snow melting periods, and the choice of temporal resolution of the inflow measurements. For inflow, there is often, depending on the time resolution, a significant degree of autocorrelation from one period to the next. E.g., after a period of precipitation or snow melting, one is likely to experience consecutive days and weeks of increased inflow. A significant degree of autocorrelation favors the use of autoregressive processes. In EOPS, the inflow for a local system is assumed to follow an ARIMA(1,1) process. Maceira and Damázio (2006) propose a periodic autoregressive process (PAR) for inflow in the Brazilian hydropower system. Since PAR allows for negative inflows and do not account for the skewness of the inflow distribution very well, Shapiro et al. (2013) propose to use geometric PAR models (GPAR). In GPAR, the deviations of the log inflows from their periodic mean are represented as an AR(1) process. We will adopt this approach in this paper.

For hydropower dominated systems, multiple papers show that there exists a general a negative correlation between inflow and the electricity price, e.g., Mo et al. (2001). Naturally, when reservoir levels are low, prices increase as a result of lower supply. The nature and strength of this correlation will depend on several factors. Among these is the choice of time resolution, and whether we look at local or system-level inflow. All else equal, one will expect the strength of the relationship to be stronger for a coarse granularity of time (e.g., quarterly or yearly data), as the impact on the supply will be more substantial for inflow aggregated over a longer time.

The inflow-price relationship is in varying degree taken into account in the literature and commercial software. Kolsrud and Prokosch (2010) found a relationship between the spot price, the overall aggregated reservoir level in a given geographical area and the local reservoir level of a single plant. Further, EMPS, which is used to find spot price scenarios to be used in EOPS, finds spot price as a function of aggregated, regional inflow. On the contrary, Fosso et al. (1999) show that EOPS treats movements in local inflow and price as independent variables. Intuitively, we would expect the correlation between price and inflow to be stronger on an aggregated national level, than between the local inflow of a particular power plant and the system price. However, we do not expect local inflow and price to be independent. This is because the local inflow can be heavily correlated with the aggregated national inflow, as found in Boger et al. (2017). Therefore, we include a correlation between movements in local inflow and the price of forward contracts in the stochastic processes.

The paper is organized as follows. In Section 2, we present the reservoir management decision problem as a mathematical program. We also give an overview of the stochastic processes used to describe the correlated movements of inflow and price and how these can be used to generate a scenario lattice. The section is concluded with a short description of ADDP, the framework used to solve the decision problem. In Section 3, we present a multi-reservoir hydropower plant in Norway on which we have tested our model. We also present the obtained process coefficients and correlation, and show empirical results from running the model. The section is concluded with a calculation of the losses associated with using a single factor price

process and from omitting the price-inflow correlation. Final conclusions are made in Section 4.

2 Methods

In the following sections, we will first formulate the decision problem associated with reservoir management as a mathematical program. Then, we will show how movements in the two relevant stochastic variables, spot price and inflow, can be modeled. Further, we present how all future states of price and inflow can be discretized using a scenario lattice, and briefly present the solution method used to obtain optimal decision policies for each state.

2.1 Hydropower decision problem

In this part, we describe the problem faced by a price-taking hydropower production planner with multiple, interconnected reservoirs that participates in deregulated market. Based on a broad set of endogenous and exogenous variables such as reservoir level, inflow and spot price, they must decide how much water they should use for power production in a given period and how much they should store for future production. The production planner is limited by multiple constraints, e.g., on reservoir volume and turbine capacity, and his primary concern is how they can utilize their water to maximize the expected present value of all discounted future cash flows.

The problem faced by the production planner is a stochastic dynamic decision problem, meaning that decisions must be made at different stages in time and in light of uncertainty about future states of their environment. For each time step, there are two stochastic, exogenous variables that affect the decisions of the production planner; spot price P_t and inflow $Y_{b,t}$ into all reservoirs $b = [1,...,B]$. For convenience, we denote $\hat{Y}_t = \{Y_{b,t} : b = [1,...,B]\}$ as a set of all inflows to all reservoirs at time t. Like Bjerksund et al. (2008), we assume that the decision maker participates in a complete market with no riskless arbitrage opportunities. Harrison and Pliska (1981) define a complete market as a market where the price of all securities is attainable, and there exists only one single price for each security. In a complete and arbitrage-free market, there would exist a unique risk-neutral, martingale measure $\mathbb{Q}$ that represents the risk-neutral probabilities of all future states for spot price and inflow.

Using the complete market and no-arbitrage assumption and denoting π_t as a decision policy at time t providing a cash flow of $CF_t = CF_t(P_t, \hat{Y}_t, \pi_t)$ and an appropriate discount factor $\beta_t < 1$, the expected discounted cash flows over a time horizon $\hat{T}$ are given by

$$\max_{\pi_t} \quad \mathbb{E}_{\mathbb{Q}}\Big(\sum_{t=1}^{\hat{T}} \beta_t CF_t(P_t, \hat{Y}_t, \pi_t)\Big) \tag{1}$$

Like Lamond and Boukhtouta (1996), we treat the reservoir management problem as a Markov decision process (MDP). The objective of MDPs is to obtain optimal decision policies (π_t) for all current and future states of the world. These policies maximize the value of all current and future cash flows, meaning that the policies do not only depend on their respective states, but also the space of potential future states. We denote by V_t the time t value of the current time cash flow and all future expected cash flows, and formulate it using the Bellman equation, first introduced by Bellman (1957)

$$V_t(P_t, \hat{Y}_t, \pi_t) = \max_{\pi_t} \quad CF_t(P_t, \pi_t) + \beta_t \mathbb{E}[V_{t+1}(P_{t+1}, \hat{Y}_{t+1}, \pi_{t+1} | P_t, \hat{Y}_t, \pi_t)] \tag{2}$$

Equation (2) is a recursive formula, meaning that the time t value of all future cash flows V_t is a function of the immediate cash flows CF_t and the expected next step value V_{t+1}. The possible values of V_{t+1} are, however, dependent on the current time decisions, indicating the importance of choosing π_t such that it does maximize not only the current cash flow, but also all expected future cash flows.

In hydropower production, the cash flows earned by the production planner equal the product of spot price and the amount of produced energy. When ignoring turbine and generator start-up costs, which is quite common in other papers discussing hydropower reservoir management (e.g., Wallace and Fleten, 2003), cash flows can be set equal to revenues. Thus, (2) can be considered as the objective function of the decision problem. For a hydropwer system consisting of B interconnected reservoirs, we denote by $w_{bi,t}$ the amount of water in $[m^3]$ nominated for production in a turbine connecting reservoir b and reservoir i. In case the nominated water flows into an outlet (e.g., a river, lake or fjord), we set $i = O$. Further, ς and ϖ are the number of seconds and hours, respectively, the plant's turbines are running per week. Given that the plant produces at constant rate, we can define $q_{bi,t} = w_{bi,t}/\varsigma$ as the water discharge in $[m^3/s]$ from reservoir b flowing into reservoir i at time t. Further, we let $H_{b,t}$ denote the head elevation in reservoir b, and $\eta_{bi,t}$ the efficiency rate of a turbine connecting reservoir b and i. In reality, these are typically functions of multiple decision variables, e.g., reservoir volume and water discharge. While we do not define these functions now, we discuss their form further in Section 3.2. Lastly, given a water density ρ and gravitational acceleration G, the cash flow CF_t at time t can be written as

$$CF_t = P_t \cdot \rho \cdot G \cdot \varpi \cdot \sum_{b \in B} \Big[H_{b,t} \cdot \sum_{i \in B, i \neq b} q_{bi,t} \cdot \eta_{bi,t} \Big] \quad t = [1,...,\hat{T}] \tag{3}$$

We denote by $l_{b,t}$ the water level in $[m^3]$ in reservoir b at time t. Further, $u_{bi,t}$ is the amount of water flowing from reservoir b to reservoir i outside a turbine, that is, either through a

regulated channel or as spillage. Like above, we set $i = O$ if the water flows into an outlet. The general volume balance of all reservoirs will then be given by

$$l_{b,t} = l_{b,t-1} - \sum_{i \in B, i \neq b} [w_{bi,t} + u_{bi,t}] + Y_{b,t} + \sum_{i \in B, i \neq b} u_{ib,t} \quad t = [0, ..., \hat{T}], \quad b = [1, ..., B] \quad (4)$$

Further, the problem faces multiple restrictions. All reservoirs are subject to a minimum and maximum level of water, denoted by $\underline{l_{b,t}}$ and $\overline{l_{b,t}}$. These limits can be based on physical constraints such as reservoir geometry and dam robustness, but also on government regulations, some of which may be seasonal. There are also restrictions in the turbines, stating the maximum allowed water discharge $\overline{q_{bi}}$ that they can handle. In case there exists no turbine at reservoir b whose water flows into reservoir i, $\overline{q_{bi}}$ will logically be 0. Finally, due to infrastructural reasons (e.g., too small channels or insufficiently robust spillways), there might be a maximum constraint on the allowed amount of water flowing from reservoir b to i, $\overline{u_{bi,t}}$. If no water can flow from reservoir b to i, either due to the lack of physical connections or the effects of gravity (the head elevation of reservoir i is higher than that of reservoir b), $\overline{u_{bi,t}}$ will logically be 0. All these constraints can be summarized in (5)-(8).

$$l_{b,t} \leq \overline{l_{b,t}} \quad \text{for} \quad t = [1, ..., \hat{T}], \quad b = [1, ..., B] \quad (5)$$

$$l_{b,t} \geq \underline{l_{b,t}} \quad \text{for} \quad t = [1, ..., \hat{T}], \quad b = [1, ..., B] \quad (6)$$

$$q_{bi,t} \leq \overline{q_{bi}} \quad \text{for} \quad t = [1, ..., \hat{T}], \quad b = [1, ..., B], \quad i \in B, i \neq b \quad (7)$$

$$u_{bi,t} \leq \overline{u_{bi,t}} \quad \text{for} \quad t = [1, ..., \hat{T}], \quad b = [1, ..., B], \quad i \in B, i \neq b \quad (8)$$

By combining all expressions and restrictions, our dynamic program can be summarized as solving the following mathematical program at time t

$$\begin{aligned} &\max && V_t(P_t, \hat{Y}_t, \pi_t) \\ &\text{subject to} && (4), (5), (6), (7), (8) \end{aligned}$$

2.2 *Electricity price process*

We model spot price movements as a Markov process and use the price of forward contracts to forecast future spot prices. At time t, $F_{t,T}$ is the price of a forward contract traded in a market with maturity (or delivery) at time T. For a forward contract with immediate delivery ($T = t$), the price of that contract is simply the current time spot price, that is $P_t = F_{t,t}$. Thus, a stochastic process for the price development of forward contracts with different times to maturity can be used to represent future spot prices. In a liquid power market, the available future and forward contracts traded at time t should represent the current time risk-adjusted market expectations for future spot prices, meaning that the spot prices projected by the process will incorporate these expectations. A further advantage is that the price of all forward contracts traded in the market include the seasonality of electricity prices, an important characteristic of electricity spot prices, as described by Johnson and Barz (1999). This implies that the process does not need any deterministic function to account for seasonality.

As stated previously, we want to use a multi-factor process to describe movements in price. Including multiple factors should allow the process to better explain the real dynamics driving forward price movements, and thereby make better price predictions. Such a process can be formulated as a multi-factor extension of the HJM model, originally presented by Heath et al. (1992). An HJM model with I sources of uncertainty is given by

$$\frac{dF_{t,T}}{F_{t,T}} = \sum_{i=1}^{I} \sigma_{i,t,T} dZ_{i,t} \quad (9)$$

Here, $\sigma_{i,t,T}$ is the ith volatility function of a forward contract with maturity at time T, and $dZ_{i,t}$ is a source of uncertainty where $Z_{i,t}$ follows a Wiener process. Together, $\sigma_{i,t,T}$ for $i = [1, ..., I]$ explain the dynamics driving the time t movement of a forward contract with maturity at time T. The ith volatility function is associated with the ith source of uncertainty, $dZ_{i,t}$. Since our decision problem considers discrete time stages, (9) must be discretized. By using Ito's lemma and setting $dt = \Delta t$, the process can be written as

$$F_{t,T} = F_{t-\Delta t,T} \cdot \exp\Big(- \frac{1}{2} \sum_{i=1}^{N} \sigma_{i,T-t+\Delta t}^2 \Delta t + \sum_{i=1}^{N} \sigma_{i,T-t+\Delta t} \sqrt{\Delta t} \varepsilon_{i,t} \Big) \quad (10)$$

Here, $\Delta Z_{i,t} = \sqrt{\Delta t} \varepsilon_{i,t}$ where $\varepsilon_{i,t} \sim N(0,1)$. Using $P_t = F_{t,t}$, we can modify (10) into an expression for the spot price P_t as a function of $F_{t-\Delta t,t}$, given by

$$P_t = F_{t,t} = F_{t-\Delta t,t} \cdot \exp\Big(- \frac{1}{2} \sum_{i=1}^{N} \sigma_{i,\Delta t}^2 \Delta t + \sum_{i=1}^{N} \sigma_{i,\Delta t} \sqrt{\Delta t} \varepsilon_{i,t} \Big) \quad (11)$$

2.3 Estimating the volatility functions of the price process

In the literature, multiple ways are proposed on how the volatility functions in (9) can be obtained. Koekebakker and Ollmar (2005) propose that they can be found empirically as a function of time to maturity, that is, on the form $\sigma_{i,t,T} = \Psi_i(T-t)$. In order to do so, we must construct a sufficiently large dataset of daily returns for multiple types of forward contracts $m = [1,...,M]$ with time to maturity $\tau_m = T - t$. Using τ as time to maturity, the volatility functions can be denoted $\sigma_{i,\tau}$. In order to calculate these returns series, Koekebakker and Ollmar (2005) propose constructing multiple forward curves for a large set of historical trading days and then calculate daily returns as the deviations between two consecutive curves.

In the Nordic power market, tradable forward and future contracts have delivery periods stretching over longer time periods. A forward curve is a curve that aims to explain the expected forward price for delivery in each hour/day/week in a time interval (t_b,t_e) based on all contracts available in the market whose delivery periods span the interval. A forward curve constructed on the date t_s is denoted $f(t_s)$. $f(t_s,t)$ where $t > t_s$ denotes the value of that curve for time t, and intends to represent the price of a fictional forward contract with delivery exactly at time t. Multiple ways of constructing forward curves are presented in the literature, e.g. by Fleten and Lemming (2003), Benth et al. (2007), Alexander (2008) and Kiesel et al. (2017). After constructing a set of curves for multiple consecutive days, we can use (12) to calculate daily returns at time t_j for contracts with time to maturity τ_a. This is a modified version of the method used by Koekebakker and Ollmar (2005), as we choose to calculate continuously compounded logarithmic returns rather than discrete compounded returns. We do this because it allows us to calculate returns over longer time periods by addition, thereby simplifying many calculations. This approach is also used by Bjerksund et al. (2008).

$$x_{j,a} = \ln(f(t_j, t_j + \tau_a)) - \ln(f(t_{j-1}, t_j + \tau_a)) \tag{12}$$

Here, $j = [2,...,J]$ and $a = [1,...,A]$, where J is the number of forward curves and A is the number of maturity dates for which we want to construct a dataset. The returns series matrix calculated using $J+1$ forward curves (meaning we can find J returns) and A different time to maturities is then given by

$$\mathbf{X_{J\times A}} = \begin{bmatrix} x_{1,1} & x_{1,2} & \dots & x_{1,A} \\ x_{2,1} & x_{2,2} & \dots & x_{2,A} \\ \vdots & \vdots & \ddots & \vdots \\ x_{J,1} & x_{J,2} & \dots & x_{J,A} \end{bmatrix} \tag{13}$$

Having found $\mathbf{X_{J\times A}}$, we use principal component analysis (PCA) to find the desired I volatility functions. PCA is an orthogonalization technique used to reduce the dimensionality of a dataset consisting of highly correlated variables. Mathematically, the principal components of $\mathbf{X_{J\times A}}$, whose correlation matrix is denoted $\mathbf{V}$, are given by $\mathbf{P} = \mathbf{X_{J\times A}W}$. Here, $\mathbf{W}$ is a matrix whose columns are the eigenvectors $\mathbf{w_i}$ of $\mathbf{V}$ sorted in descending order based on their corresponding eigenvalue λ_i. As shown in Clewlow and Strickland (2000), the volatility functions will then be given by $\sigma_{i,\tau_a} = \sqrt{\lambda_i} w_{ai}$, where $i = [1,...,A]$.

To reduce the dimensionality, we only include the volatility functions associated with the first I principal components. Typically, one would choose I such that the proportion of variance explained by the first I factors is around 90%-95%. Clewlow and Strickland (2000) show that only two components are needed to explain 96.8% of total variation of NYMEX crude oil futures contracts, whereas Koekebakker and Ollmar (2005) needed more than ten components to explain the same proportion for Nordic electricity forwards in the period 1995-2000.

2.4 Inflow process

The inflow process is based on the geometric periodic autoregressive (GPAR) model presented by Shapiro et al. (2013). The authors found that a first-order periodic autoregressive process of the log-inflows provides a good description of the dataset, which contained inflow observations from the Brazilian hydropower system. They found that the distribution of inflow observations Y_t is highly right-skewed. Therefore, they work with $\ln(Y_t)$ to obtain a distribution with less skew.

Let $\hat{\mu}_t$, $t = 1,...,52$ be the weekly averages of $\ln(Y_t)$ and $W_t = \ln(Y_t) - \hat{\mu}_t$ be the corresponding deviations. Shapiro et al. (2013) found that W_t could be described by an AR(1) process. (14) shows how the deviations of the log inflows from their mean can be described as an 1-lag autoregressive process.

$$W_t = \phi_0 + \phi_1 W_{t-1} + \varepsilon_{Y,t} \tag{14}$$

Here, ϕ_0 and ϕ_1 are parameters of the process, and $\varepsilon_{Y,t}$ is the error term representing the difference between the observed and predicted value. To be able to model the inflow as a stochastic process, we assume that the error terms are distributed $\varepsilon_{Y,t} \sim N(0, \sigma_Y^2)$, where σ_Y is the standard deviation of the error terms. The parameters ϕ_0 and ϕ_1 are estimated by ordinary least squares regression. Because W_t observations are themselves deviations, ϕ_0 is highly insignificant. We set $\phi_0 = 0$ and use $\phi_1 = \phi$ from this point on. Next, we find the log inflow, $W_t + \hat{\mu}_t$

$$\begin{aligned} W_t + \hat{\mu}_t &= \phi W_{t-1} + \varepsilon_{Y,t} + \hat{\mu}_t \\ &= \phi(W_{t-1} + \hat{\mu}_{t-1}) - \phi\hat{\mu}_{t-1} + \varepsilon_{Y,t} + \hat{\mu}_t \end{aligned} \tag{15}$$

The inflow Y_t can be expressed as a function of $W_t + \hat{\mu}_t$.

We insert the obtained expression of $W_t + \hat{\mu}_t$ into $Y_t = \exp(W_t + \hat{\mu}_t)$, and get

$$Y_t = \exp(W_t + \hat{\mu}_t) = \exp(\phi Y_{t-1}) \exp(-\phi \hat{\mu}_{t-1} + \varepsilon_{Y,t} + \hat{\mu}_t) \quad (16)$$

By rewriting, we obtain the inflow process described by (18).

$$Y_t = \exp(\phi \ln Y_{t-1}) \exp(\hat{\mu}_t - \phi \hat{\mu}_{t-1} + \varepsilon_{Y,t}) \quad (17)$$

$$Y_t = \exp(\varepsilon_{Y,t}) \exp(\hat{\mu}_t - \phi \hat{\mu}_{t-1}) Y_{t-1}^{\phi} \quad (18)$$

We further allow the error term standard deviation σ_Y and the coefficient ϕ to be time-dependent. The final inflow process can then be expressed as

$$Y_t = \exp(\varepsilon_{Y,t} + \hat{\mu}_t - \phi_t \hat{\mu}_{t-1}) Y_{t-1}^{\phi_t} \quad (19)$$

where t is the week number and $\varepsilon_{Y,t}$ now follows the distribution $\varepsilon_{Y,t} \sim N(0, \sigma_{Y,t}^2)$. Since inflow Y_t is a function of its first lag only, future values of inflow are only dependent on their current value and not the entire history. Thus, inflow also follows a Markov process, which was one of the prerequisites for representing our decision problem as a Markov decision process.

2.5 Scenario lattice for spot price and inflow

To solve the MDP, we must discretize the exogenous Markov process that describes inflow and price movements. As in Löhndorf and Wozabal (2017), we do this by reducing the continuous Markov process to a discrete scenario lattice. In our case, each lattice node represents a state of both reservoir inflow and spot price. Generally, we keep the number of nodes per stage in the lattice constant. In comparison, the number of nodes per stage in a scenario tree grows exponentially with the number of time stages. Thus, the lattice approach allows for a greater number of time stages while still keeping the problem computationally feasible.

In order to construct a lattice, we use the method proposed by Löhndorf and Wozabal (2017). We denote N_t as the number of nodes at time t. Further, $\overline{S_{tn}} = \{P_{tn}, Y_{tn}\}$ denotes the nth state (or node) at time stage t, where P_{tn} is the state spot price and $Y_{tn} = \{I_{b,tn} : b = [1,...,B]\}$ is a set of inflows into all B reservoirs for the same state. We also let $n \in [N_t]$, where N_t is the total number of states at time t. In short, the lattice is constructed by first drawing a set of K Monte-Carlo simulations ($\hat{S}^k$) of spot price and inflow, where $\hat{S}_t^k = \{P_t^k, Y_t^k\}$ is the time t state of simulation k where $k \in [K]$. These simulations are drawn using (11) for the spot price and (19) for inflow, where the error terms $\varepsilon_{i,t}$ and $\varepsilon_{Y,t}$ are correlated with ρ_i. Afterwards, the location of all states $\overline{S_{tn}}$ is found by minimizing the Wasserstein distance between all N_t nodes and the K simulated draws $\hat{S}_t^k$ for each time stage t. Having located all nodes, the transition probabilities between two subsequent nodes $\overline{S_{tn}}$ and $\overline{S_{t+1,m}}$ can be found by looking at the number of simulated paths whose time t and $t+1$ states lie closest to the nodes $\overline{S_{tn}}$ and $\overline{S_{t+1,m}}$.

2.6 Solution method for optimization problem

We adopt the method known as approximate dual dynamic programming (ADDP) to find the near optimal decision policies π_{tn} in all nodes of the price and inflow lattice. ADDP was first introduced by Löhndorf et al. (2013). In principle, obtaining optimal decision policies for a Markov decision process should be possible using traditional dynamic programming (DP) as introduced by Bellman (1957). Using the notation introduced in Section 2.5, the Bellman equation given in (2) can then be rewritten into

$$V_t(\overline{S_{tn}}, \pi_{tn}) = \max_{\pi_{tn}} \quad CF_t(\overline{S_{tn}}, \pi_{tn}) + \beta_t \mathbb{E}[V_{t+1}(S_{t+1}, \pi_{t+1} | \overline{S_{tn}}, \pi_{tn})] \quad (20)$$

A common problem with dynamic programming is the curse of dimensionality. It has been addressed by multiple authors, i.e. by Powell (2011). In this case, the main issue with a high-dimensional problem is that the decision space can become too large to find the optimal decisions for all states within a reasonable amount of time. We must, therefore, use a method that resolves this issue by obtaining decision policies that are approximately optimal. Multiple such methods are proposed in the literature, and they are often referred to as approximate dynamic programming. A method that has been widely used to manage hydropower reservoirs is stochastic dual dynamic programming (SDDP), first introduced by Pereira and Pinto (1991). Löhndorf et al. (2013) extend the method of SDDP so that it can also be used for scenario lattices, calling it ADDP. When using SDDP and ADDP, one of the main simplifications is that the value function V_t is approximated to be a piece-wise linear, concave function of all resource variables (e.g., reservoir levels). In short, the value function is found by first drawing a given number of *forward passes* through the lattice, that is, a sequences of states. For each forward pass, the optimal decision policies are found by maximizing the approximate post-decision value functions. After each forward pass, a *backward pass* is performed, where the approximated value functions are updated relative to the sampled sequence of states and all state decision policies. In practice, the approximate value function of each state is constructed by a set of supporting hyperplanes (linear constraints), where each pair of forward and backward passes results in the addition of a new hyperplane to the set. For a more detailed description of the ADDP algorithm, consult Löhndorf et al. (2013).

3 Results

In this section, we summarize the results of a case study conducted with data from a Norwegian hydropower producer. The Søa hydropower plant is presented in Section 3.1. In Section 3.2, we discuss the decision problem. Section 3.3 discusses the characteristics of the price process and its associated volatility functions. Then, we present the parameters of the inflow process in Section 3.4 and the price and inflow correlation in Section 3.5. Section 3.6 shows how we construct the scenario lattice using correlated Monte Carlo simulations. We present the expected revenues by applying the scheduling model in Section 3.7. In Section 3.8, we perform a backtest of our model compared to historical operations. Further, in Section 3.9 we analyze potential differences and losses in expected revenues with regards to different values of the price-inflow correlation. We perform a similar analysis in Section 3.10, considering the case were the number of factors I used in the forward price process is altered. All code and calculations are produced in MATLAB and R, except for the algorithms used to construct a lattice and the ADDP solver.

3.1 Case: Søa hydropower plant

We have received empirical data from the Søa hydropower plant, a plant owned and operated by the integrated electric utility company TrønderEnergi. Apart from sharing the relevant characteristics of the plant, TrønderEnergi has also provided us with historical time series for inflow and production. The plant is mid-sized both in terms of regulating capacity and power capacity, and it is located in the NO3 area in Norway. It consists of two reservoirs - Vasslivatn and Søvatn, and one Francis turbine. The discharge from the Søvatn reservoir to the Vasslivatn reservoir is controllable. In Table 2, we have listed the physical boundaries of both reservoirs. There is also a special summertime restriction that applies for Søvatn, which is set by local authorities. This restriction and its duration are also listed in Table 2. The outlet of the hydropower plant is in Hemnefjorden, which has an average head of -1 MASL (meters above sea level).

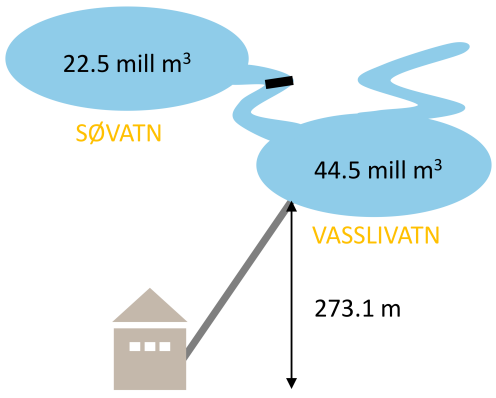

Figure 1: The Søa hydropower plant and the reservoir capacities. The elevation of 273.1m is the production-weighted average head difference between Vasslivatn and Hemnefjorden.

Table 1: Characteristics of the Søa hydropower plant

	Value	Unit
Maximum power capacity	36	MW
Mean yearly production	191.3	GWh
Avg. yearly inflow, total	311	mill m^3
Average inflow to Søvatn	60.5	% of total
Average inflow directly to Vasslivatn	39.5	% of total
Energy coefficient	0.6748	kWh/m^3
Turbine capacity	17	m^3/s

The energy coefficient listed in Table 1 takes into account all sources of energy loss in the system, including head loss, turbine losses, generator losses and transformer losses. It is calculated using the production-weighted average head elevation (273.1 m) and production-weighted average discharge to the turbine.

Table 2: Water level constraints for Søa. All water levels are denoted in meters above sea level

Reservoir	Restriction type	Min [MASL]	Max [MASL]
Vasslivatn	Physical	260.00	279.83
Søvatn	Physical	275.00	279.83
Søvatn	Regulatory (May 25 - Oct. 15)	278.33	279.83

3.2 Revised decision problem

In order to construct the lattice mentioned earlier and perform ADDP on Søa hydropower plant, we use QUASAR, a general purpose solver for stochastic optimization (Löhndorf and Wozabal, 2017). To keep computation complexity at bay, we use a linear reformulation of the problem.

The number of reservoirs is $B = 2$, and we let $l_{1,t}$ and $l_{2,t}$ denote the water levels in Vasslivatn and Søvatn respectively. Also, $Y_{1,t}$ and $Y_{2,t}$ denote the inflows into each reservoir. Since the system only contains one turbine which connects Vasslivatn to the outlet of Hemnefjorden, we denote the amount of water nominated for production as w_t and its discharge as q_t. The amount of water flowing from Søvatn to Vasslivatn (denoted $u_{12,t}$ using notation from Section 2.1) is now denoted by u_t, and the amount of spilled water flowing from Vasslivatn to Hemnefjorden is denoted by s_t (previously denoted $u_{1O,t}$). With these new notations, the general volume balance constraint from (4) can be written as (21) and (22) for Vasslivatn and Søvatn, respectively.

$$l_{1,t} = l_{1,t-1} - w_t - s_t + Y_{1,t} + u_t \quad \text{for} \quad t = [1,...,\hat{T}] \tag{21}$$

$$l_{2,t} = l_{2,t-1} + Y_{2,t} - u_t \quad \text{for} \quad t = [1,...,\hat{T}] \tag{22}$$

Neither u_t nor s_t are restricted by an upper bound $\overline{u_{ij,t}}$, so this constraint is omitted from the revised problem formulation. Due to the linearity requirement, the cash flow

expression CF_t defined by (3) can only be a function of one decision variable. While head elevation, turbine and generator efficiency are typically functions of one or more decision variables, we must model them as constants in order to keep the expression linear. Such simplifications are made in similar models for reservoir management, e.g., EOPS (SINTEF, 2017b). Madani and Lund (2009) also use a fixed head and argue that this is a reasonable assumption for high-elevation hydropower systems. There is no formal definition of high-elevation plants, but they typically have a head elevation above 250-300 meters. As the head elevation of Søa is within this interval, it is not highly unreasonable to argue for using a constant head. Also, if the head is chosen as the centre of gravity for the reservoir (i.e., about 270 MASL, indicating an elevation of 271 meters between the reservoir and the outlet), the deviations between realized power and approximated power will be in the range $[-3.7\%, 3.7\%]$. We believe this is acceptable, considering the granularity of our model.

When we use constant values for head elevation and efficiency rate, the objective function of the optimization problem consists of many constants whose product is the energy coefficient. By definition, the energy coefficient is the average amount of energy a hydropower plant can produce by using one cubic meter of water. In the objective function, we, therefore, make the simplification $\rho GH\eta\varpi/\varsigma = \kappa$, where κ denotes the energy coefficient.

Further, we only have available data on the aggregated inflow into both reservoirs, forcing us to treat inflow as a single stochastic variable $Y_t = Y_{1,t} + Y_{2,t}$. In order to obtain $Y_{1,t}$ and $Y_{2,t}$, we have used the historical inflow split given in Table 1. We let $\alpha = 0.395$ denote the historical fraction of inflow flowing into Vasslivatn, and thereby set $Y_{1,t} = \alpha Y_t$ and $Y_{2,t} = (1-\alpha)Y_t$. Also, since the water level in Søvatn is subject to a minimum restriction during the summer $l_{2,t} > 0$, we must include a slack variable $l^S_{2,t}$ to account for cases in which this constraint cannot be held. Since we do not know the exact cost of violating the constraint, we add a sufficiently large cost Υ associated with the slack variable to the value function such that its value is kept at a minimum. By combining all the mentioned simplifications and adjustments, our optimization problem at time t is reduced to

$$
\begin{aligned}
\max \quad & V_t = P_t \cdot \kappa \cdot w_t - \Upsilon \cdot l^S_{2,t} \\
& + \beta_t \mathbb{E}[V_{t+1} | P_t, Y_t, \pi_t] \\
\text{subject to} \quad & l_{1,t} = l_{1,t-1} - w_t - s_t + \alpha Y_t + u_t \\
& l_{2,t} = l_{2,t-1} + (1-\alpha) Y_t - u_t \\
& l_{1,t} \leq \overline{l_{1,t}} \\
& l_{2,t} \leq \overline{l_{2,t}} \\
& l_{1,t} \geq \underline{l_{1,t}} \\
& l_{2,t} + l^S_{2,t} \geq \underline{l_{2,t}} \\
& q_t \leq \overline{q}
\end{aligned}
$$

where $\pi_t = \{w_t, l_{1,t}, l_{2,t}, u_t, s_t, l^S_{2,t}\}$. All coefficients and constant parameter values are given in Table 3. We recall that water discharge is defined as $q_t = w_t/\varsigma$ where ς is the number of seconds of production per week. The larger we choose ς, the larger becomes the maximum limit for w_t, water nominated for production at time t. In cases of large inflows, low values for ς will only result in larger amounts of spilled water, indicating that ς should be set as large as possible. Also, since efficiency rate is not modeled as a function of water discharge q_t, the choice of ς will be irrelevant for the value function in all stages where spillage is of no concern. We, therefore, set $\varsigma = 604800s$, which is the total number of seconds in one week. Furthermore, we find the time-dependent discount factor β_t using the risk-free rate r given by the Norwegian Interbank Offered Rate (NIBOR). To get comparable results between runs for different days, we chose to use a constant value of r (NIBOR for 6-month maturity debt on January 7, 2013). Optimally, we would have used an estimate of the two-year maturity risk-free rate, but six months was the longest maturity available. The discount factor β_t is found using continous compounding, given by $\beta_t = \exp(-rt)$.

Table 3: Model coefficients and constants

Coefficient/ Parameter	Value	Unit	Dates
$\overline{l_{1,t}}$	44.5	Mm^3	$t = [1,...,\hat{T}]$
$\overline{l_{2,t}}$	22.5	Mm^3	$t = [1,...,\hat{T}]$
$\underline{l_{1,t}}$	0	Mm^3	$t = [1,...,\hat{T}]$
$\underline{l_{2,t}}$	0	Mm^3	$t =$[October 16,...,May 24]
$\overline{l_{2,t}}$	15.05	Mm^3	$t =$[May 25,...,October 15]
κ	0.6747	kWh/m^3	$t = [1,...,\hat{T}]$
ς	604800	s	$t = [1,...,\hat{T}]$
$\overline{q}$	17	m^3/s	$t = [1,...,\hat{T}]$
r	0.0198	$-$	$t = [1,...,\hat{T}]$

3.3 Electricity spot price and forward curve dynamics

The first step towards obtaining the volatility functions describing the forward curve dynamics is to construct historical forward curves. They are found by interpolating between forward prices as described by Alexander (2008). The dataset of this study includes forward prices for all trading days between April 28, 2011, to December 30, 2016, resulting in 1450 forward curves. The forward curves are constructed using closing prices of futures contracts traded at NASDAQ Commodities. These contracts are listed in Table 4.

Table 4: Electricity forward contracts traded on NASDAQ Commodities

Code	Length of delivery period	Trading period
ENOW	Week	1, 2, 3, 4, 5, 6 weeks ahead
ENOM	Month	1, 2, 3, 4, 5 and 6 months ahead
ENOQ	Quarter	1, 2, 3, 4, 5, 6, 7 and 8 quarters ahead
ENOYR	Year	1, 2 and 3 years ahead

Figure 2 shows the forward curve found for January 7, 2013. It is clear that the forward curves found using this method

will be discontinuous in the points where we switch from one contract type to another, as illustrated in Figure 2. As can be seen in Figure 2, weekly contracts was used in the short end of the curve, monthly contracts in the mid-short part of the curve, quarterly contracts in the mid-long part of the curve, and yearly contracts in the long end of the curve.

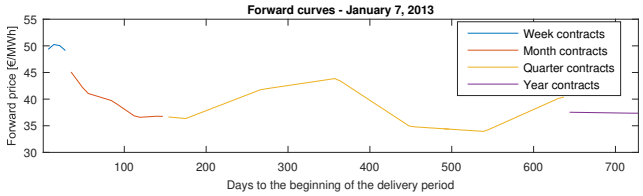

Figure 2: Forward curve created using linear interpolation

A time series of daily log returns is calculated for each relevant time to delivery, resulting in a 1449×104 matrix. To obtain a set of volatility functions that describe forward price movements, PCA is used on the returns time series as explained in Section 2.2. Remember that each volatility function is associated with an independent uncertainty factor. The volatility function determines by how much, and in which direction the random shock associated with the uncertainty factor moves each point of the forward curve. As we use weekly granularity and a time horizon of 105 weeks, the volatility functions $\sigma_{i,\tau} = \Psi_i(\tau)$ must be constructed for the same granularity and length. That is, we find the volatility functions $\sigma_{i,\tau}$ for all $i = [1,...,N]$ and time to maturity given by $\tau = [1,2,...,104]$ weeks.

Using the time series of returns, we can estimate an overall volatility curve for the term structure of forward prices, as well as the volatility functions associated with the principal components. In Figure 3, the overall volatility function can be understood as the volatility of returns of forward contracts with time to maturity τ. Since it represents the actual volatility of forward price returns, it will always be positive. The volatility functions associated with the principal components must, however, not be interpreted the same way as the overall volatility function, as they do not represent the volatility in terms of price movements of a single asset. They can also take negative values, as opposed to the overall volatility function.

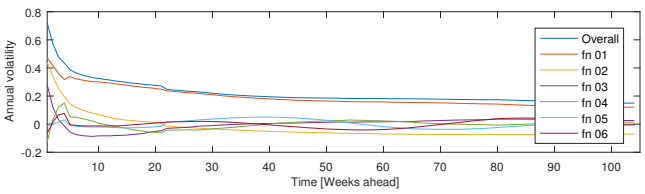

Figure 3: Volatility functions found by using method of linear interpolation. 'Overall' denotes the overall volatility curve, and fn i denote the volatility functions given by principal component i

As can be seen from the dark blue curve in Figure 3, the overall volatility is *monotonically decreasing*. One would expect the overall volatility function to be strictly decreasing for ascending values of τ, as forward prices tend to change more the closer they come to maturity. This is called the *Samuelson effect*, discussed by Jaeck and Lautier (2016) and originally proposed by Samuelson (1965). The reasoning behind this phenomenon is that an information shock that affects the short-term price has an effect on the succeeding prices that decreases as the time to maturity increases. Weather forecasts are an example of information that one would expect to have short-term effects only on the electricity price.

The electricity forward return series show a substantial degree of inter-correlation. This can be seen from the correlation matrix that is shown in Figure 4. A high degree if inter-correlation is in accordance with our experience, which is that forward electricity prices more often than not move in the same direction. Further, the correlation matrix shows that there is a clear decreasing trend in the correlation between contracts with larger maturity spreads.

The high degree of inter-correlation is also demonstrated by the explanatory power of the first principal component, which explains 73.3% of the variance in the dataset. Only six principal components are needed to explain over 95% of the cumulative variance, as shown in Table 5.

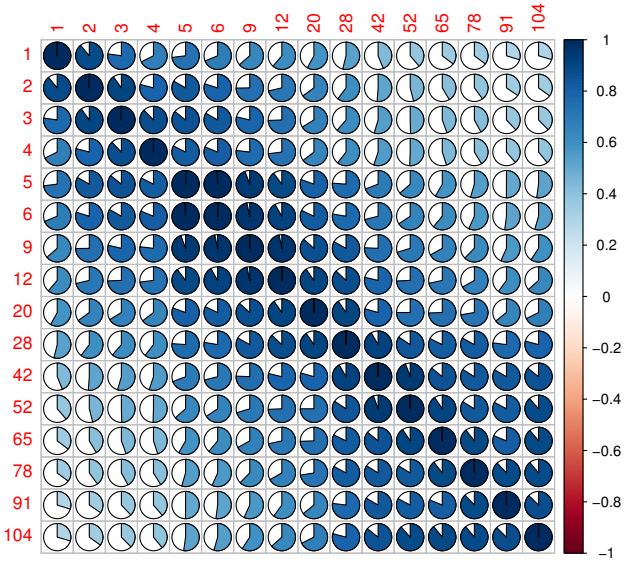

Figure 4: Correlation matrix associated with returns of forward contracts. The column and row names are both the number of weeks until the beginning of the delivery period

Table 5: Proportion of explained variance for different numbers of explanatory factors

Number of factors n	1	2	3	4	5	6
Explained variance	0.73	0.88	0.92	0.93	0.95	0.96

3.4 *Inflow process parameters*

We fit the geometric periodic autoregressive (GPAR) model suggested by Shapiro et al. (2013) to the inflow data for the Søa hydropower plant. The dataset consists of daily inflow observations for each day between January 1, 1958, and December 31, 2016. According to TrønderEnergi, the data set has been constructed by combining observations from two different sources. The observations from the most accurate source are found by measuring the change in water level at the reservoirs and finding the inflow by adjusting for water used in production and spilled water. For days without available production data, the inflow is calculated by measuring the water level in the rivers in the catchment area of the hydropower plant.

Recall that the inflow is given by

$$Y_t = \exp\left(\varepsilon_{Y,t} + \hat{\mu}_t - \phi_t \hat{\mu}_{t-1}\right) Y_{t-1}^{\phi_t} \tag{19}$$

Here,

- Y_t is the inflow in week t
- $\hat{\mu}_t$ is the mean log inflow in week $t = 1, \ldots, 52$
- ϕ_t is the coefficient in the autoregressive process in week $t = 1, \ldots, 52$
- $\varepsilon_{Y,t} \sim N(0, \sigma^2_{Y,t})$ is the error term representing the difference between the observed and predicted value in the autoregressive process
- $\sigma_{Y,t}$ is the standard deviation of the error terms in week $t = 1, \ldots, 52$

For a right-skewed distribution such as the one that can be seen in Figure 5, a geometric process is better suited than an arithmetic process. It better captures the inflow dynamics, which can be extreme. Further, a geometric process does not allow for negative inflows. Shapiro et al. (2013) found the inflow distribution for Brazilian hydropower plants to be right-skewed as well, favoring a log transformation of the inflow observations.

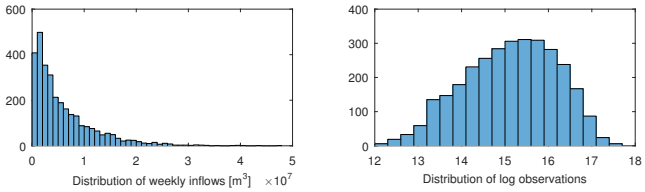

Figure 5: Distribution of inflow and log inflow observations

W_t, the deviation of the log inflows from their mean, is represented as an AR(1) process. The suitability of a 1-lag process can be determined by investigating the partial autocorrelation of the historical data for W_t. Partial autocorrelation is the correlation for a time series with its own lagged variables, but removing the correlation effects of the values of the time series at all shorter lags. Figure 6 shows the partial autocorrelation of the W_t time series. Similar to the findings of Shapiro et al. (2013), our dataset showed a high value at lag 1 and insignificant values for larger lags, indicating that it is sufficient to include one lag only in the autoregressive model.

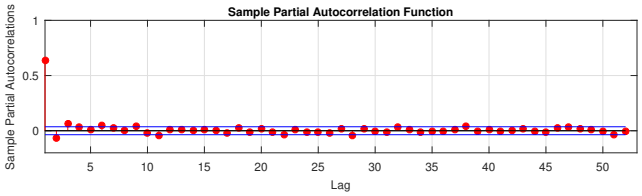

Figure 6: Partial autocorrelation of the W_t time series

The inflow process is periodic in the sense that it accounts for seasonality - both in terms the expected weekly log inflow $\hat{\mu}_t$, the strength of the autoregressive coefficient (ϕ_t) and the standard deviations of the error terms ($\sigma_{Y,t}$). Figure 7 shows the seasonal pattern in the inflows. Specifically, there is an inflow peak during the spring due to snow melting, and there are higher inflow levels in the fall due to high precipitation levels in September, October, and November.

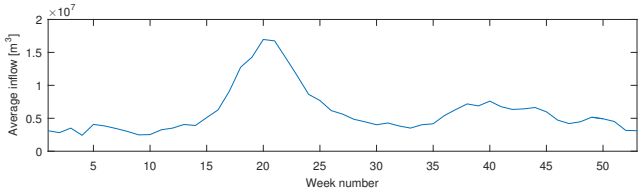

Figure 7: Average inflow for a certain week of the year

3.5 *Price and inflow correlation*

As previously mentioned, we consider the correlation between the electricity spot price and inflow to the hydropower plant. In Section 2.5, this was introduced as the correlation ρ_i between the error terms $\varepsilon_{i,t}$ and $\varepsilon_{Y,t}$ from Equation (11) and (19), where $i = [1, \ldots, I]$ indicates a principal component. Since the first principal component explains 73.38% of the total variation, we choose only to calculate ρ_i for $i = 1$, and set $\rho_i = 0$ for $i \neq 1$. Therefore, ρ_1 is hereby denoted ρ. Mathematically, the correlation was calculated by estimating the historical correlation coefficient between the normalized error term of the inflow process, $\varepsilon_{Y,t}$, and the normalized first principal component ($\mathbf{p}_1$).

The error term in the inflow process is the difference between the predicted and realized log-inflow. To be able to find a correlation with the weekly inflow data, $\mathbf{p}_1$ had to be transformed into a weekly resolution as well. Similar to how one would transform daily log returns to weekly log returns, the historical $\mathbf{p}_1$ observations were aggregated from daily to weekly observations by simple addition.

The resulting Pearson correlation coefficient was found to be -0.1765, based on a time series of 248 weekly

observations from April 28, 2011, to December 30, 2016. The 95% confidence interval was [-0.28, -0.06]. This suggests that there has been a weak offsetting effect between weekly inflow deviations and the first principal component, historically.

3.6 Monte Carlo simulations and lattice construction

In order to create a lattice, we had to run multiple parallel Monte Carlo simulations of spot price and inflow paths. The starting values of the price simulations included one current time spot price and the price of $\hat{T}-1$ forward contracts. Since we use weekly granularity and a horizon of $\hat{T}=105$ weeks, this requires 104 weekly forward contracts with time to delivery $\tau=[1,...,104]$. However, only six weekly contracts are traded at NASDAQ Commodities, meaning that we must construct 99 synthetic weekly contracts. This is done by constructing a forward curve using the method of Fleten and Lemming (2003) and then discretizing it into 104 weekly prices. Unlike the forward curves used to construct the volatility functions, which were discontinuous (see Figure 2), forward curves constructed using the method of Fleten and Lemming (2003) are both continuous and smooth. The method did, however, not provide us with plausible volatility functions, as we experienced issues with unrealistic oscillations in the near end for some of the forward curves.

Mathematically, the forward price of a contract with delivery in a given week $W=[2,...,105]$ is calculated using the average value of the forward curve within the time interval of that particular week. For the weeks $W=[2,...,7]$, the weekly average value of the forward curve will be the price of the six weekly forward contracts sold in the market. Also, if the model is run on a Monday, the starting week spot price is set equal to the price of the one week ahead weekly contract from the last trading day. Typically, this will be the previous week Friday.

It is important to note that while the spot prices in the Nordic electricity market are area specific, the price of forward contracts is the same for the entire Nordic and Baltic region. Thus, the spot price forecasted by our model is actually the system spot price and not the NO3 area spot price, the price Søa hydropower plant receives for their production. In this paper, have not tried to model the relationship between the system price and the NO3 price. We do, however, see that the two prices are quite similar to each other, and believe that using the system price instead of the area price is an acceptable approximation considering the granularity and the scope of this paper.

To construct the price and inflow scenario lattice, we have used 380.000 Monte Carlo simulations. The lattice consists of 100 nodes for all time stages except the starting one, giving a total count of 10401 nodes. Furthermore, each node has two entries, inflow and spot price. Figure 8(a) displays the spot price lattice with starting date January 7, 2013, while Figure 8(b) displays the inflow lattice. Since the lattice nodes are found by minimizing the Wasserstein distance, we have scaled the inflow values down with a factor of 10^5 such that their magnitudes are closer to those of the spot prices.

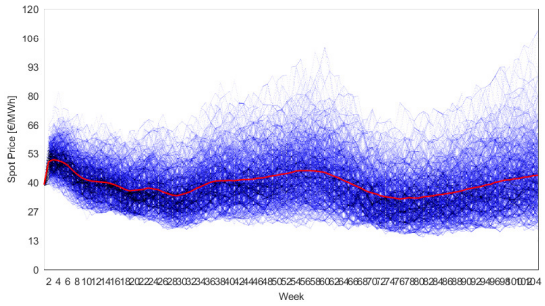

(a) 105-weeks spot price lattice

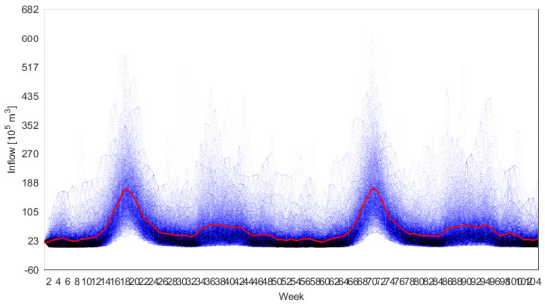

(b) 105-weeks inflow lattice

Figure 8: Spot price and inflow lattices constructed with data for January 7, 2013. The Y-axis for all plots denotes the time stages (weeks), while the X-axis of the price lattice is denotes the spot price in EUR/MWh. For the inflow lattice, the Y-axis is denoted in $10^5 m^3$. The red lines in the figures represent the mean values. In the case of the spot price lattice, the mean line is the initial forward curve.

3.7 Expected discounted revenues from hydropower plant

Having constructed the lattice, it is now possible to run the scheduling model. We run it for five different starting dates with different underlying forward curves and historical starting values for the reservoir levels. One of the key figures we are interested in is the *expected discounted revenues* for the planning horizon. This is the value of production during the next two years, assuming negligible variable costs. The revenues are discounted using the risk-free rate, as we are using risk-neutral probabilities. Furthermore, a key figure is the expected discounted revenues per produced unit of electricity, which we will call *expected discounted revenues per production*. This figure is denominated in EUR/MWh, and it allows us to compare the performance of policies without differences in total production affecting the results. For intuition, this figure can be thought of as the average price at which the hydropower producer sells their power. However, this will be inaccurate in this case, since the average price should be calculated using undiscounted revenues.

Table 6 shows the expected discounted revenues for the upcoming 105 weeks, in addition to the expected discounted revenues per production. These results are based on

the revenues obtained by 50.000 simulated paths through the lattice. The number (50.000) is chosen because it enables the first three digits of all mean values to converge, while simultaneously keeping the computation time at an acceptable level.

In Table 6, we also include one of the most important immediate results for the production planner; the value of w_1. We recall that w_t is the amount of water nominated for production at time stage t. Based on all possible future states and their corresponding probabilities, w_1 tells the production planner how much water they should nominate for production in the current week in order to maximize their expected discounted revenues over the upcoming 105 weeks. We also include the average water dispatch $q_1 = w_1/\varsigma$, where $\varsigma = 604800s$ is the number of seconds per week.

Table 6: Expected discounted revenues (EDR), expected discounted revenues per production (EDR/Prod.), the amount of water nominated for production w_1, and average water discharge q_1 in week one for five different starting dates. The starting values for reservoir levels are set according to their historical values.

Parameter	Unit	Jan 7 2013	Apr 8 2013	Jul 8 2013	Oct 7 2013	Jan 6 2014
EDR	[M EUR]	15.93	15.95	14.36	15.26	13.83
EDR/Prod.	[EUR/ MWh]	40.12	41.24	35.35	38.36	33.21
w_1	[M m^3]	0	5.21	10.28	0	0
q_1	$[m^3/s]$	0	8.62	17.00	0	0

It is somewhat surprising that the model suggests no production on multiple starting weeks, especially those of January 7, 2013, and January 6, 2014. However, this is because the input forward curve suggests that the spot prices will be higher in the upcoming weeks, making it optimal to wait.

An important question that arises is how one should handle the end level of the reservoir. We have not imposed any end level restrictions. Thus, there is no incentive to keep water in the reservoir at the end of the horizon. In some of the above simulations, e.g., the ones starting and ending in January, emptying the reservoir would probably be a poor decision in the reality since one would normally expect high prices in the upcoming periods. Emptying the reservoirs in the last time stage will result in expected discounted revenues that are slightly larger than what one would achieve in reality. Nevertheless, the end-of-horizon effects should not affect the optimal immediate decision policy π_1, which is the most interesting one for the production planner, in addition to most decision policies π_{tn} when t is substantially smaller than 2 years. Note that for cases in which the time horizon ends during the spring when inflows are typically at their maximum, it is reasonable to allow emptying the reservoir as much as possible.

3.8 Backtesting the production policy with realized price and inflow data

A crucial analysis for assessing the performance of the scheduling model is a backtest. When backtesting, we have collected the realized weekly inflows and average area spot prices over the entire simulation horizon. Then, we apply the policy to the realized history of price and inflow and get all decisions that our model would have made for the given history of inflow and price. Using this, we can compare how our model performs compared to the existing strategies of the hydropower production planner. Using January 7, 2013, as our starting date, we have found the realized weekly inflows and spot prices over the next 105 weeks. Next, we have found the total revenues earned using the model policy, and compare this with the actual income earned by the power plant in the same time interval. In reality, the Søa power plant generated discounted revenues of *10.89 million EUR* between January 7, 2013, and January 11, 2015, from trading in the spot market. By applying the policy obtained by our model, the plant would have had discounted revenues of *11.69 million EUR*, meaning that using our model could have provided the production planner with approximately 400.000 EUR in extra yearly revenues. To explain this difference, we look at the modeled and realized head elevation curves for both reservoirs in the corresponding period. These are interesting to compare, as they show whether the model policy agrees or disagrees with the realized strategy. In Figure 9 we have plotted the modeled and realized head curves for both reservoirs over the simulation period.

By visual inspection, we see that our model empties both reservoirs in the last time stage, providing it with some additional revenues compared to the historical operations. Thus, it might be more accurate to compare the revenues obtained during the first 52 weeks - that is, between January 7, 2013, and January 5, 2014, instead. In this period, the plant earned discounted revenues of *6.22 million EUR*. On the contrary, using the policies from our model, the discounted revenues provided to the plant would be *6.34 million EUR*, meaning that our model performs well compared to reality also without emptying the reservoir in the last time stage. Our model did, however, utilize more of its water for production in these 52 weeks, so we should also compare the expected discounted revenues per production as well. In reality, the plant had discounted revenues per production of *39.00 EUR/MWh* between January 7, 2013, and January 5, 2014, while our model had discounted revenues per production of *38.92 EUR/MWh*.

Further inspection of the head curves shows that our model is less risk-averse than the real-life production planner. One example of this can be seen by looking at the figure for Vasslivatnet around week 36, that is, in the middle of September 2013. Here, spot prices were quite high, so both our model and the real-life operation planner chose to nominate relatively large amounts of water for production. However, since spot prices tend to be higher during winter, it is risky to empty the reservoirs in September. Therefore,

the real-life production planner chooses to nominate only half of the amount that the model nominates. The model is, however, expecting high inflows in the upcoming weeks, and therefore nominates relatively much water before it fills up the reservoir around week 46. Another good example is around week 71, that is, one week before the summertime restriction on the reservoir level in Søvatnet starts to apply. While the real-life production planner fills up Søvatnet a few weeks ahead, the model expects sufficient inflows during the next week and decides to reduce the water level in the reservoir to approximately 1 meter below the summertime restriction. It does, however, still manage to fill up the reservoir and meet the constraint in time.

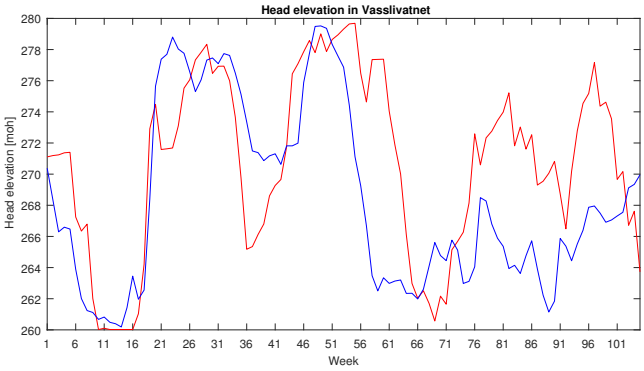

(a) Vasslivatnet

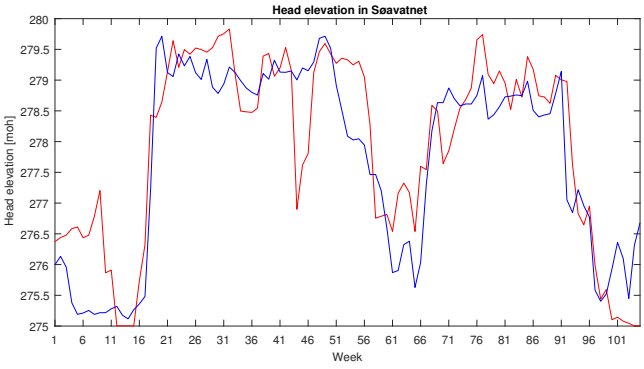

(b) Søvatnet

Figure 9: Modelled (red curve) and realized (blue curve) reservoir curves for Vasslivatnet and Søvatnet between January 7, 2013 and January 11, 2015.

The aforementioned points should help our model perform better than the real-life production planner. Another factor helping our model is that it does not have to perform maintenance, which is an event that forces all operation to be temporarily suspended. However, the real-life production planner has an advantage that our model does not have. Since our model uses weekly granularity, it can only make production decisions on a weekly basis. We assume that our model sells the electricity at a price equal to the average price of that week. In real life, the production planner makes hourly decisions and can utilize the fluctuations of the electricity spot price both within a single day and within a week. They do also have access to the intraday market, allowing them to optimize their production further. The opportunity to optimize production on an hourly level should give the real-life production planner an advantage compared to our model. At last, the real-life production planner has access to short-term weather forecasts the our model does not. Despite the circumstances discussed above, our model still manages to achieve similar results.

3.9 Loss calculations: Misspecified correlation coefficient

As previously stated, we incorporate a correlation between movements in price and local inflow. It is interesting to test the effect of introducing this feature, as it can tell us how models that assume no correlation perform compared to ours. Therefore, we have first calculated the expected revenues obtained when using different values of the correlation coefficient ρ. More importantly, we have also tested how decision policies obtained using $\rho = 0$ perform when inflow and price movements are in fact correlated, and what losses in expected a plant can experience when this assumption is falsely made.

In order to test the effect of introducing the correlation, we have first made three lattices with different correlation values $\rho = [0, -0.1765, -0.353]$. We then compare the simulated expected discounted revenues and average reservoir level curves for all three lattices and corresponding decision policies to see how much they deviate. Once again, we have used 50.000 simulated paths, and for all three runs, the starting date is January 7, 2013. The expected discounted revenues of all three runs are displayed in Table 7 and mean optimal reservoir curves for Vasslivatn are displayed in Figure 10.

Table 7: Expected discounted revenues (EDR) obtained using three different correlation coefficients ρ.

Correlation coefficient	[-]	$\rho = 0$	$\rho = -0.18$	$\rho = -0.35$
EDR	[M EUR]	16.10	15.93	15.83

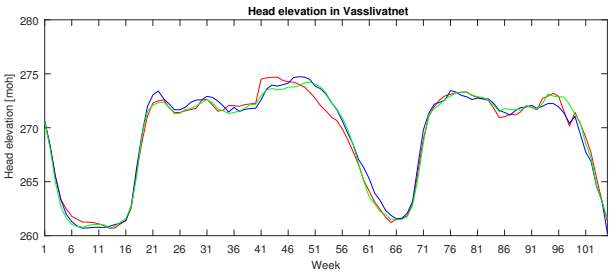

Figure 10: Average reservoir curves for Vasslivatnet found using three different values of the correlation coefficient ρ. The red curve denotes $\rho = 0$, the blue curve $\rho = -0.1765$ and the green curve $\rho = -0.353$.

By looking at the expected discounted revenues, we see that the higher we choose the correlation coefficient ρ, the larger are the expected discounted revenues. The correlation coefficient undoubtedly affects the results, implying that it must be estimated correctly.

Next, we test how a decision policy created using the

correlation $\rho = 0$ performs when we use it in a stochastic process where $\rho \neq 0$. We test this by first creating a lattice and obtaining the optimal decision policies for each node using $\rho = 0$. Instead of drawing simulated lattice paths based on the risk-neutral probabilities provided when $\rho = 0$, we draw paths corresponding to a stochastic price and inflow process where $\rho \neq 0$. Then, to compare the policies, we look at the difference between the expected discounted revenues obtained using policies with $\rho = 0$ and policies with $\rho \neq 0$. In Table 8, we present the expected discounted revenues obtained when the stochastic processes in reality have a correlation $\rho = -0.1765$ and $\rho = -0.353$. As the results indicate, if the real correlation is $\rho = -0.1765$, the policies will provide expected discounted revenues that are 2.5% lower than if the policies incorporated this correlation. For $\rho = -0.353$, the expected discounted revenues become 3.1% lower. Although these differences might seem small, they show that the producer at Søa can miss out on discounted revenues of multiple 100.000 EUR yearly if they misspecify the correlation coefficient. Therefore, we find it reasonable to conclude that the choice of the correlation coefficient does have an effect on the model performance, and should be considered by the production planner in their model.

Table 8: Expected discounted revenues (EDR) calculated when using a policy in which $\rho = 0$, but where the real stochastic process has $\rho = [-0.1765, -0.353]$. The bottom row indicates the difference between the expected discounted revenues obtained using these policies versus the expected discounted revenues obtained using a policy with the same ρ as in the stochastic process, as shown in Table 7.

Correlation coefficient	[-]	$\rho = -0.1765$	$\rho = -0.353$
EDR	[M EUR]	15.54	15.40
Performance difference	[-]	-2.5%	-3.1%

3.10 Loss calculations: Number of factors in the price process

Further, up until now, we have used a price process with six factors to describe the movements of a forward contract. The number was chosen such that the proportion of explained variance would be larger than 95%, a threshold value used by Koekebakker and Ollmar (2005). However, Bjerksund et al. (2008) claim that a proportion of 90% is sufficient, while Clewlow and Strickland (2000) choose the number of factors such that the proportion becomes 98.4%. Therefore, we perform a set of calculations similar to those in Section 3.9, but instead of testing different values of ρ, we use a different number of factors I in the price process. We investigate four different numbers of factors: 1 (that is, we use the overall volatility function), 3 (91.53% explanation), 6 (96.04% explanation) and 10 (98.44% explanation). The obtained expected discounted revenues are shown in Table 9, and the mean optimal reservoir levels in Figure 11.

Table 9: Expected discounted revenues (EDR) obtained using different number of factors I to describe the underlying price process.

Number of factors	[-]	$I = 1$	$I = 3$	$I = 6$	$I = 10$
EDR	[M EUR]	15.80	15.86	15.93	16.00

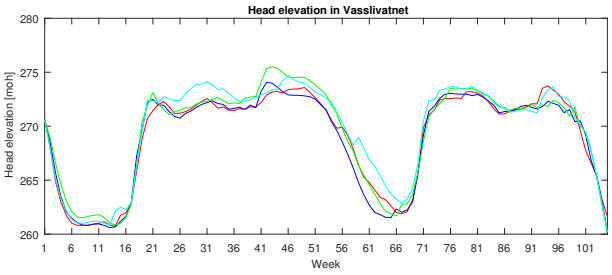

Figure 11: Average reservoir curves for Vasslivatnet obtained using different number of factors in the forward price process. The red curve is from a run with $I = 1$ factors, the dark blue one for a run with $I = 3$, the red curve for $I = 6$ and the light blue curve for $I = 10$.

The results in Table 9 show that there is an increasing trend in expected discounted revenues when we use more factors to describe the price process. This should make sense, as more factors can result in larger price fluctuations, thereby resulting in a lattice with a larger difference between the highest and lowest possible price at a time stage. The optimal policies utilize the higher prices in the lattices with more factors, and the model thereby forecasts larger expected discounted revenues.

As for the case with different values of ρ, it might be more interesting to test how the policies obtained using one-factor price model perform when the price process can, in reality, be described using $I = [3, 6, 10]$ factors. We, therefore, redo the steps explained above for the case of different numbers of factors I instead of correlation coefficient ρ. The expected discounted revenues are displayed in Table 10. By looking at the numbers, we see that a policy created using a one-factor price model will underperform by approximately 2% when the price process is in fact driven by multiple factors. Similar to the case for different values of ρ, this can result in a decrease in revenues of multiple 100.000 EUR yearly for a hydropower plant, underlining the importance of using a price process that is as correct as possible when modeling reservoir management.

Table 10: Expected discounted revenues (EDR) calculated when using a policy where the number of factors is $I = 1$, but where the real stochastic price process is described by $I = [3, 6, 10]$. The bottom row indicates the difference between the expected discounted revenues using these policies versus the expected discounted revenues obtained using a policy with the same number of factors I as in the stochastic process, as shown in Table 9.

Number of factors N	[-]	$I = 3$	$I = 6$	$I = 10$
EDR	[M EUR]	15.52	15.61	15.63
Performance difference	[-]	-2.1%	-2.0%	-2.3%

4 Conclusions

In this paper, we present a medium-term model for reservoir management. We model the problem as a Markov decision process, and use a multi-factor model to describe changes in forward and spot prices. We incorporate a short-term correlation between the local inflow model and price model and solve the resulting stochastic-dynamic decision problem using ADDP, which descretizes the Markov processes to a scenario lattice and then solves the problem by learning an outer approximation of the value function.

We find that there exists a short-term correlation between the weekly residuals of the inflow model and the increment associated with the first volatility function of the forward curve movements. Our analysis indicates that ignoring correlation can result in sub-optimal reservoir control decisions. In our case, we observe a decrease in expected revenues of 2.5% (that is, multiple 100.000 EUR yearly) if the correlation coefficient is in fact $\rho = -0.1765$.

Our analyzes also show that it is important to use multiple factors when describing price movements. The result of our case study is that solving the problem with a one-factor model when the true model has multiple factors decrease profits by about 2%. The number of factors will depend on the price data. We confirm the finding of Koekebakker and Ollmar (2005) that we need more factors than is typical of commodity price models. In our case, we use six factors which explains 96% variance.

Compared with historical production decisions, our model produced similar results, despite the fact that decisions were made in weekly granularity, whereas the planner makes planning decisions on a daily basis. Hence, using our model provides reliable production decisions if used for medium-term planning. These results are especially interesting since our model receives the average weekly price, while the real-life production planner can make decisions on an hourly basis, allowing them to produce during periods with higher prices within a particular week that are not available for our model.

References

[1] Abgottspon, H. and Andersson, G. "Medium-term optimization of pumped hydro storage with stochastic intrastage subproblems". In: *Power Systems Computation Conference (PSCC)*. IEEE, 2014.

[2] Alexander, C. *Pricing, Hedging and Trading Financial Instruments*. Vol. III. Market Risk Analysis. Chichester, West Sussex, UK: John Wiley & Sons, Ltd, 2008.

[3] Bellman, R. *Dynamic Programming*. Princeton Landmarks in Mathematics and Physics. Princeton University Press, 1957.

[4] Benth, F. E., Koekebakker, S., and Ollmar, F. "Extracting and applying smooth forward curves from average-based commodity contracts with seasonal variation". In: *The Journal of Derivatives* 15(1) (2007), pp. 52–66. DOI: 10.3905/jod.2007.694791.

[5] Bjerksund, P., Stensland, G., and Vagstad, F. "Gas Storage Valuation: Price Modelling v. Optimization Methods". 2008. URL: https://brage.bibsys.no/xmlui/bitstream/handle/11250/163949/2008.pdf?sequence=1.

[6] Boger, M., Fleten, S.-E., Pichler, A., Keppo, J., and Vestbøstad, E. M. "Backing out Expectations from Hydropower Release Time Series". In: *IAEE International Conference*. 2017.

[7] Clewlow, L. and Strickland, C. *Energy Derivatives: Pricing and Risk Management*. London, UK: Lacima Publications, 2000.

[8] Flatabø, N., Haugstad, A., Mo, B., and Fosso, O. B. "Short-term and Medium-term Generation Scheduling in the Norwegian Hydro System under a Competitive Power Market Structure". In: *EPSOM '98 Proceedings*. Switzerland: ETH Zürich, 1998.

[9] Fleten, S.-E. and Lemming, J. "Constructing forward price curves in electricity markets". In: *Energy Economics* 25(5) (2003), pp. 409–424. DOI: 10.1016/S0140-9883(03)00039-2.

[10] Fosso, O. B., Gjelsvik, A., Haugstad, A., Mo, B., and Wangensteen, I. "Generation scheduling in a deregulated system. The Norwegian case". In: *IEEE Transactions on Power System* 14(1) (1999), pp. 75–81. DOI: 10.1109/59.744487.

[11] Harrison, J. M. and Pliska, S. R. "Martingales and stochastic integrals in the theory of continuous trading". In: *Stochastic Processes and their Applications* 11(3) (1981), pp. 215–260. DOI: 10.1016/0304-4149(81)90026-0.

[12] Heath, D., Jarrow, R., and Morton, A. "Bond Pricing and the Term Structure of Interest Rates A New Methodology for Contingent Claims Valuation". In: *Econometrica* 60(1) (1992), pp. 77–105. DOI: 10.2307/2951677.

[13] Iladis, N. A., Tilmant, A., Chabar, R., Granville, S., and Pereira, M. "Optimal operation of hydro-dominated multireservoir systems in deregulated electricity markets". 2008. URL: https://www.researchgate.net/publication/228746176_Optimal_operation_of_hydro-dominated_multireservoir_systems_in_deregulated_electricity_markets.

[14] Jaeck, E. and Lautier, D. "Volatility in electricity derivative markets: The Samuelson effect revisited". In: *Energy Economics* 59 (Aug. 2016), pp. 300–313. DOI: 10.1016/j.eneco.2016.08.009.

[15] Johnson, B. and Barz, G. "Selecting stochastic processes for modelling electricity prices". In: *Energy Modelling and the Management of Uncertainty*. Ed. by Kaminski, V. Risk Books, 1999. Chap. 1.

[16] Kiesel, R., Paraschiv, F., and Sætherø, A. "On the Construction of Hourly Price Forward Curves for Electricity Prices". Aug. 2017. URL: https://papers.ssrn.com/sol3/papers.cfm?abstract_id=2845302.

[17] Koekebakker, S. and Ollmar, F. "Forward curve dynamics in the Nordic electricity market". In: *Managerial Finance* 31(6) (2005), pp. 73–94. DOI: 10.1108/03074350510769703.

[18] Kolsrud, C. W. and Prokosch, M. "Reservoir Hydropower: The value of flexibility". Master thesis. Norwegian University of Science and Technology, June 2010.

[19] Lamond, B. F. and Boukhtouta, A. "Optimizing long-term hydro-power production using Markov decision processes". In: *International Transactions in Operational Research* 3(3-4) (1996), pp. 223–241. DOI: 10.1016/S0969-6016(96)00018-4.

[20] Löhndorf, N. and Wozabal, D. "Indifference pricing of natural gas storage contracts". 2017. URL: http://www.optimization-online.org/DB_HTML/2017/02/5863.html.

[21] Löhndorf, N., Wozabal, D., and Minner, S. "Optimizing trading decisions for hydro storage systems using approximate dual dynamic programming". In: *Operations Research* 61(4) (2013), pp. 810–823. DOI: 10.1287/opre.2013.1182.

[22] Maceira, M. and Damázio, J. "Use of the PAR (p) model in the stochastic dual dynamic programming optimization scheme used in the operation planning of the Brazilian hydropower system". In: *Probability in the Engineering and Informational Sciences* 20(1) (2006), pp. 143–156. DOI: doi.org/10.1017/S0269964806060098.

[23] Madani, K. and Lund, J. R. "Modeling California's high-elevationhydropower systems in energy units". In: *Water Resources Research* 45(9) (2009). DOI: 10.1029/2008WR007206.

[24] Massé, P. *Les Reserves et la Regulation de I'Avenir dans la vie Economique*. Vol. I and II. Paris, France: Hermann, 1946.

[25] Mo, B., Gjelsvik, A., Grundt, A., and Kåresen, K. "Optimisation of hydropower operation in a liberalised market with focus on price modelling". In: *Porto Power Tech Conference*. IEEE, 2001.

[26] Mo, B., Green, T., Warland, G., and Haugstad, A. *Dokumentasjon av ny prismodell til bruk i Vansimtap, Plansddp og Beta*. Tech. rep. Trondheim, Norway: Sintef Energiforskning AS, Sept. 2000.

[27] Pereira, M. and Pinto, L. "Multi-stage stochastic optimization applied to energy planning". In: *Mathematical Programming* 52(1-3) (1991), pp. 359–375. DOI: 10.1007/BF01582895.

[28] Powell, W. B. *Approximate Dynamic Programming: Solving the Curses of Dimensionality*. Vol. 842. Princeton, New Jersey, USA: John Wiley & Sons, 2011.

[29] Rebennack, S. "Combining sampling-based and scenario-based nested Benders decomposition methods: application to stochastic dual dynamic programming". In: *Mathematical Programming* 156 (2015), pp. 343–389. DOI: 10.1007/s10107-015-0884-3.

[30] Samuelson, P. A. "Proof That Properly Anticipated Prices Fluctuate Randomly". In: *Industrial Management Review* 6(2) (1965), pp. 41–49.

[31] Shapiro, A., Tekaya, W., Costa, J. P. da, and Soares, M. P. "Risk neutral and risk averse Stochastic Dual Dynamic Programming method". In: *European Journal of Operational Research* 224(2) (2013), pp. 375–391. DOI: 10.1016/j.ejor.2012.08.022.

[32] SINTEF. *EMPS - multi area power-market simulator - SINTEF*. 2017. URL: https://www.sintef.no/en/software/emps-multi-area-power-market-simulator/.

[33] SINTEF. *EOPS - one area power-market simulator*. 2017. URL: http://www.sintef.no/en/software/eops-one-area-power-market-simulator/.

[34] Wallace, S. W. and Fleten, S.-E. "Stochastic Programming Models in Energy". In: *Handbooks in OR and MS*. Ed. by Ruszczyński, A. P. and Shapiro, A. Vol. 10. Elsevier Science B.V., 2003. Chap. 10, pp. 637–677.

[35] Wolfgang, O., Haugstad, A., Mo, B., Gjelsvik, A., Wangensteen, I., and Doorman, G. "Hydro reservoir handling in Norway before and after deregulation". In: *Energy* 34(10) (2009), pp. 1642–1651. DOI: 10.1016/j.energy.2009.07.025.